Supplementary Information

Supplementary Figures

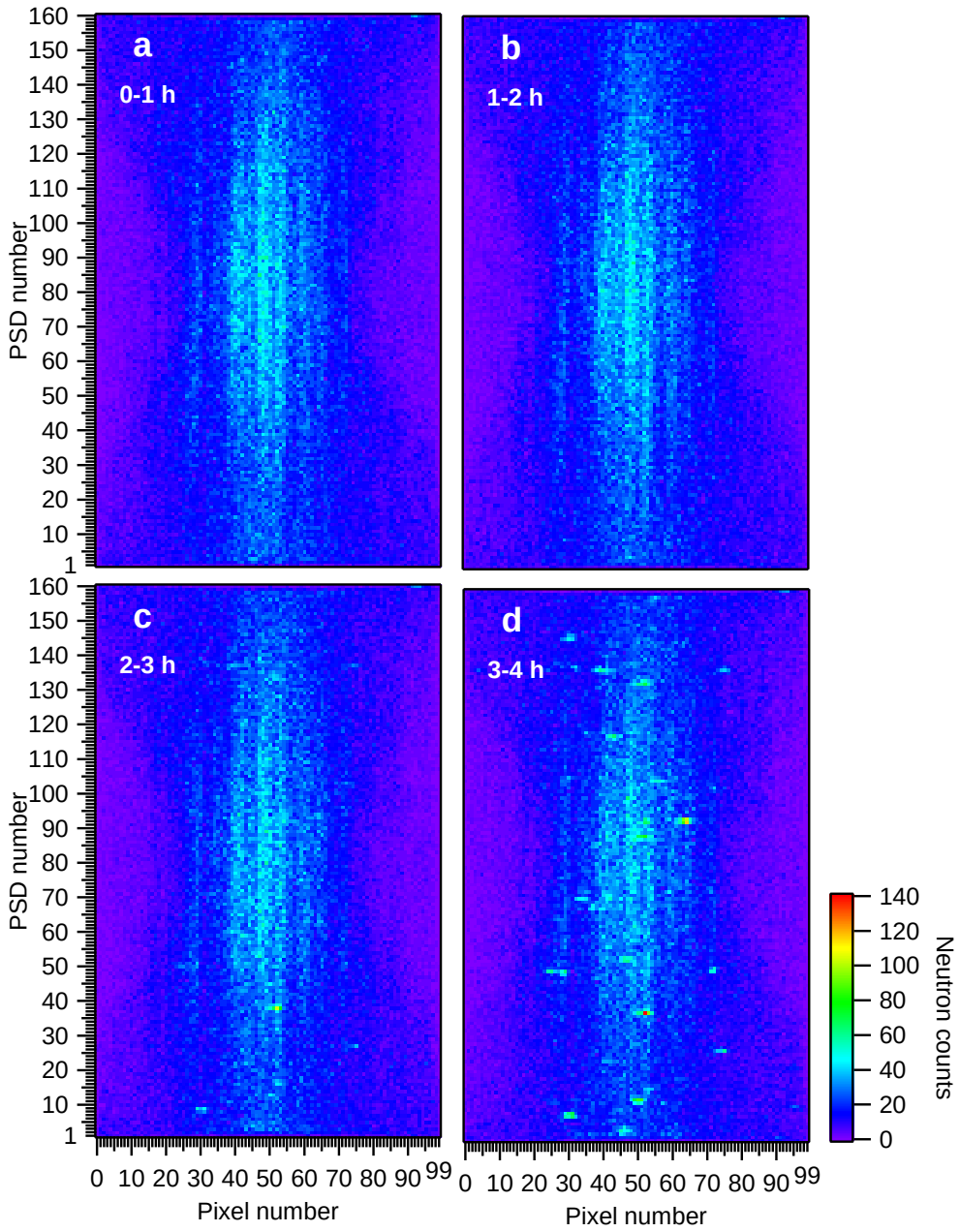

Supplementary Figure 1: Two-dimensional diffraction images recorded on the position-sensitive detector of a 90-degree bank. Time evolution of the two-dimensional diffraction images of fcc-FeD_x collected at 988 K and 6.3 GPa: (a) 0–1 h image, (b) 1–2 h image, (c) 2–3 h image, and (d) 3–4 h image. No bright spots have been recorded in the 0–1 h image, while they begin to appear in the 1–2 h image and apparently gradually increase in number in the 2–3 h and 3–4 h images.

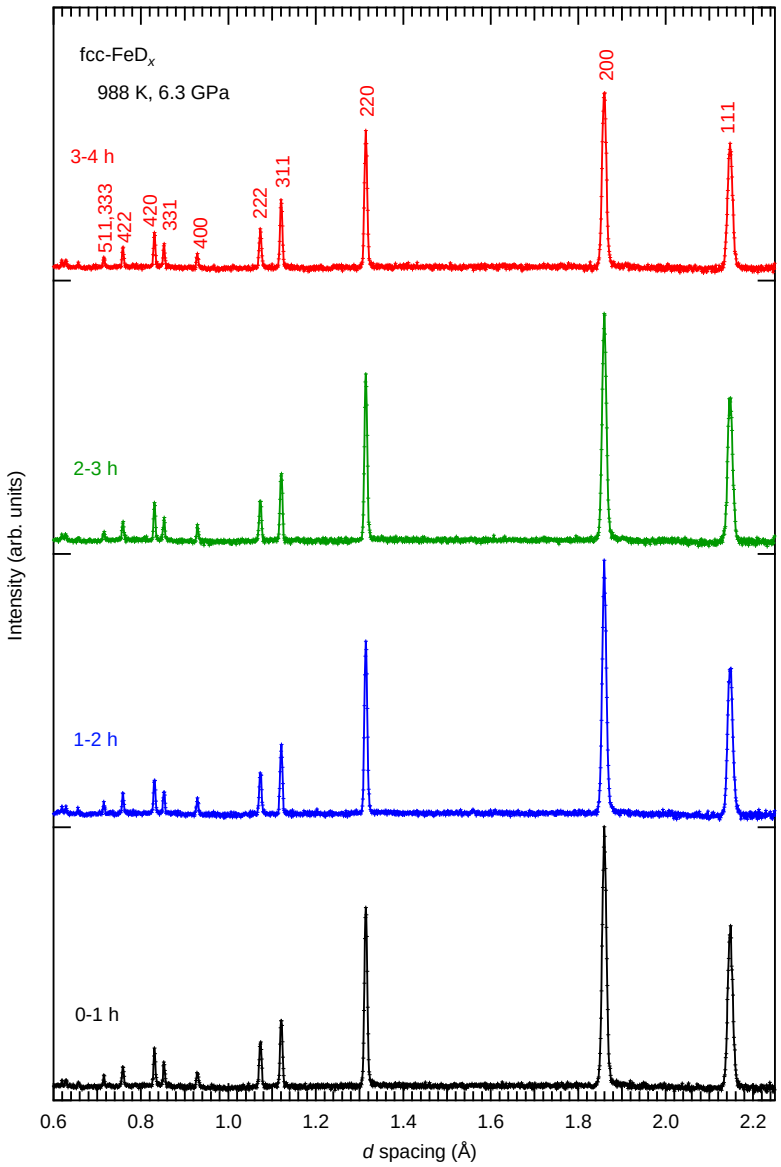

Supplementary Figure 2: Time evolution of the diffraction profile. Time evolution of the diffraction profile of fcc-FeD$_x$ at 988 K and 6.3 GPa converted from the two-dimensional diffraction images shown in Supplementary Fig. 1: 0–1 h, 1–2 h, 2–3 h, and 3–4 h profiles from the bottom to top. The 0–1 h and 1–2 h profiles are almost identical, while the peak intensities slightly decrease in the 2–3 h profile and dramatically decrease in the 3–4 h profile. The changes in the diffraction profile are attributed to grain growth. Since the 0–1 h profile is free from grain growth, it was used for the structural analysis of the equilibrium state of fcc-FeD$_x$. To confirm quantitatively the influence of the grain growth, Rietveld refinement was performed for each profile. The results of the refinements are summarized in Supplementary Table 1.

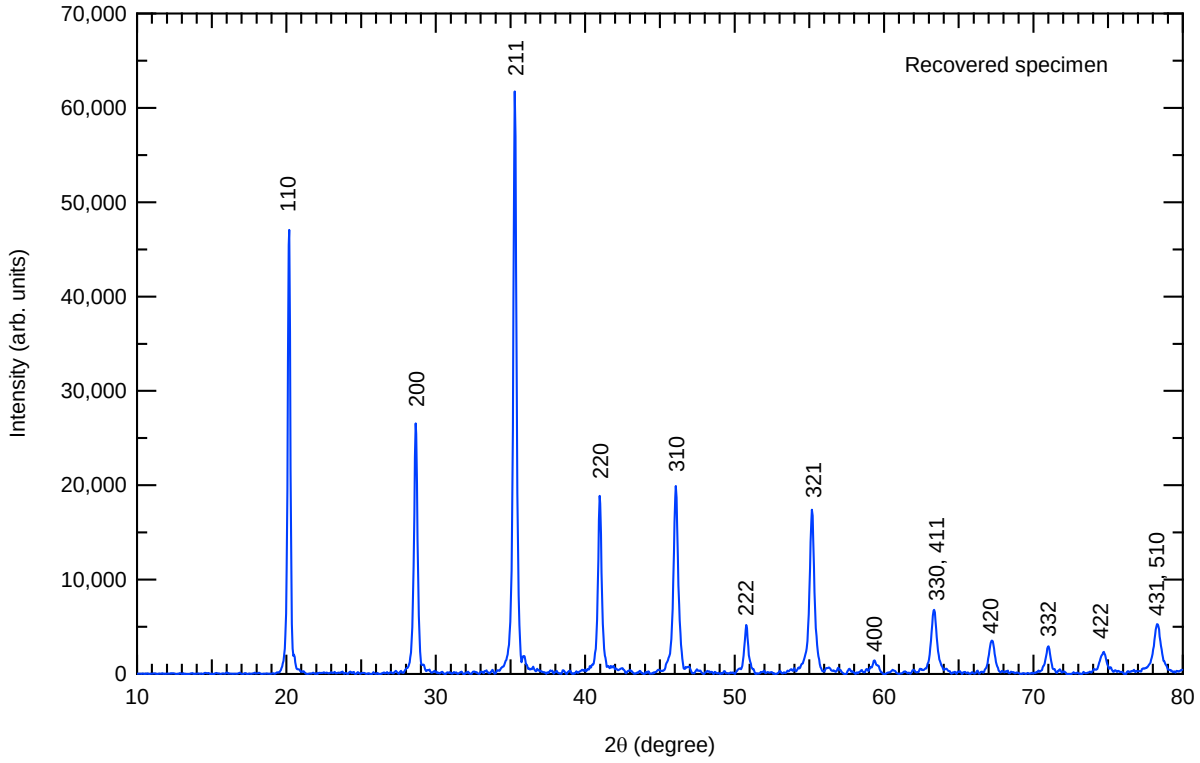

Supplementary Figure 3: X-ray diffraction profile of recovered specimen at ambient conditions using molybdenum K_α-radiation source. All reflection peaks are well indexed with a bcc lattice of iron and no reflection peak from impurity is found. The lattice constant is in agreement with that of the starting material of iron within the experimental accuracy. The reflection peaks below 30 degrees show intensities weaker than the calculated ones. This arises from the diffraction geometry of a micro X-ray diffractometer used for the recovery experiment.

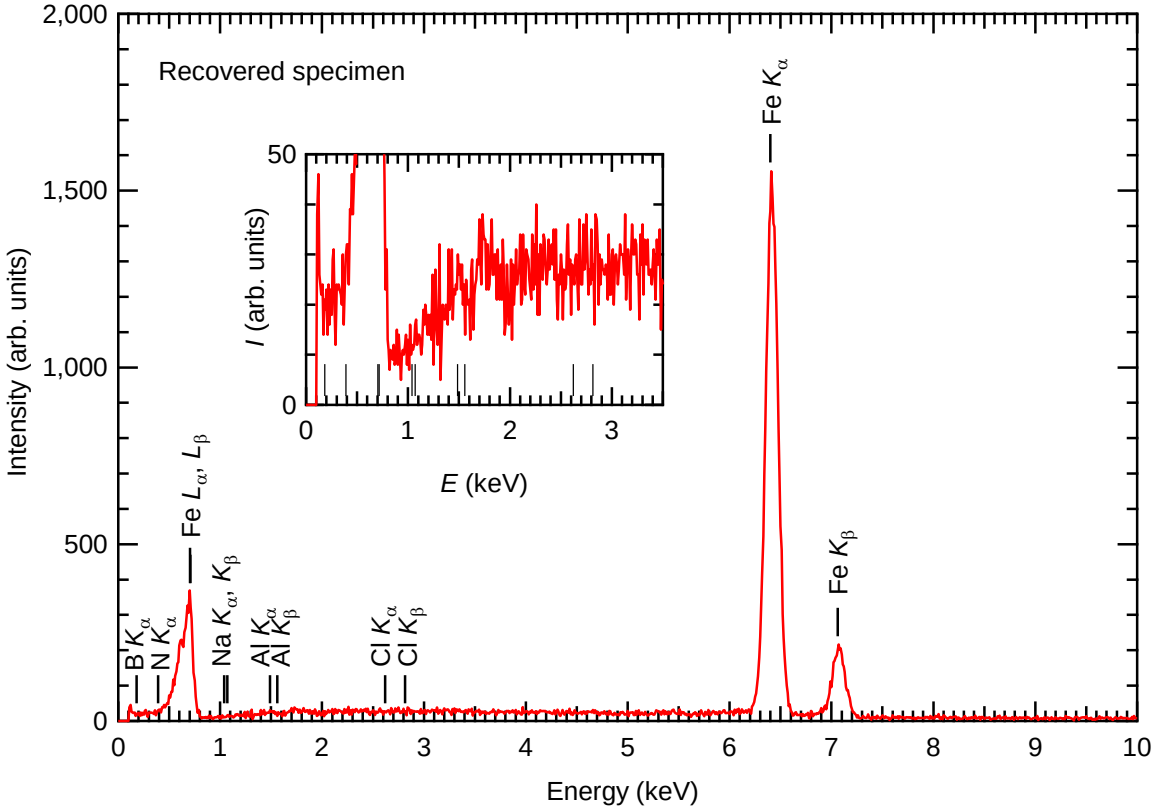

Supplementary Figure 4: EDX spectrum of recovered specimen. Three peaks are assigned to the *L*-emission line (~0.7 keV), K_α (~6.4 keV) and K_β-emission line (~7 keV) of iron, respectively. Possible atomic contaminants are Al from the AlD_3 deuterium source, Na and Cl from the NaCl deuterium sealing capsule, and B and N from the BN separator inserted between the Fe specimen and deuterium source (Figure 5). Inset is a magnified spectrum in the low energy region. Vertical bars denote the energies of emission lines of iron and possible contaminations. No detectable peak is observed for these possible contaminants within the detection limits of the EDX system operated at an accelerating voltage of 25 keV: 7000, 6000, 1000, 1000, and 1000 ppm for B, N, Na, Al, and Cl, respectively.

Supplementary Table

Supplementary Table 1: Fit results of Rietveld refinement for time evolutional diffraction profiles. Lattice parameter a, site occupancies $g_{D(O)}$ and $g_{D(T)}$, isotropic atomic displacement parameters B_{Fe} and B_D, reliability factor R_{wp}, and goodness-of-fit χ^2 are listed. These parameters were optimized using 0–1, 1–2, 2–3, and 3–4 h diffraction profiles with the structure models 1 and 2 (see the main text). Good fit results were obtained for the 0–1 h profile free from intense diffraction spots and 1–2 h profile with a few intense spots (see Supplementary Fig. 1). We chose the results of the 0–1 h profile for discussion in the main text.

Model 1	a (Å)	$g_{D(O)}$	$g_{D(T)}$	B_{Fe} (Å^2)	B_D (Å^2)	R_{wp} (%)	χ^2
0–1 h	3.71970(5)	0.474(6)	–	1.34(2)	3.2(1)	8.86	1.22
1–2 h	3.71952(5)	0.466(7)	–	1.33(2)	3.2(1)	8.83	1.16
2–3 h	3.71943(5)	0.457(7)	–	1.24(3)	3.1(1)	9.42	1.28
3–4 h	3.71918(6)	0.427(8)	–	0.94(3)	3.1(2)	9.42	1.23
Model 2	a (Å)	$g_{D(O)}$	$g_{D(T)}$	B_{Fe} (Å^2)	B_D (Å^2)	R_{wp} (%)	χ^2
0–1 h	3.71968(5)	0.532(9)	0.056(5)	1.44(3)	4.1(2)	8.47	1.12
1–2 h	3.71950(5)	0.524(9)	0.054(5)	1.44(3)	4.1(2)	8.46	1.06
2–3 h	3.71943(5)	0.52(1)	0.057(5)	1.38(3)	4.1(2)	9.06	1.18
3–4 h	3.71917(6)	0.51(1)	0.061(6)	1.05(3)	4.3(2)	9.13	1.16

Supplementary Methods

Analyses of recovered specimen

Chemical analysis and X-ray diffraction (XRD) measurements for the recovered specimen were conducted at ambient conditions. The specimen was deemed a radiation hazard after neutron irradiation and was left for several weeks until radiation intensity fell to low levels acceptable for handling. XRD measurement was performed using a micro X-ray diffractometer with a molybdenum target. Monochromatized molybdenum K_{α}-radiation X-rays were collimated into 100 μmϕ and impinged into the specimen. Diffracted X-rays were recorded on an imaging plate. Elemental analysis was conducted using a scanning electron microscope equipped with an energy dispersive X-ray spectrometer (SEM-EDX). Accelerating voltage of electron beam was 25 keV and measured area was about 50 × 50 μm^2. The lower-limit energy of the EDX measurement was approximately 0.11 keV. XRD profile and EDX spectrum were measured for the polished cut section of the recovered specimen.